

PRECIPITATION OF ENERGETIC ELECTRONS FROM THE EARTH'S RADIATION BELT STIMULATED BY HIGH-POWER HF RADIO WAVES FOR MODIFICATION OF THE MIDLATITUDE IONOSPHERE

V. L. Frolov,^{1,2*} A. D. Akchurin,² I. A. Bolotin,¹
A. O. Ryabov,¹ J. J. Berthelier,³ and M. Parrot⁴

UDC 533.95+550.348

Based on the results of the experiments performed in 2005–2010 within the framework of the Sura — DEMETER program, we analyze the features of the precipitations of energetic electrons (with energies $E \approx 100$ keV) from the Earth's radiation belt. The modification of the ionospheric F_2 region was conducted by means of high-power HF O-mode radio waves radiated in the CW regime. The precipitations were detected using the equipment onboard DEMETER, a French microsatellite. The conditions of precipitation appearance were determined, and it was found that the electron precipitation region was stretched along the geomagnetic meridian to a distance of 1300 km; the size of the region in the transverse direction is about 400 km. It was shown by ionosonde measurements that such precipitations lead to increased absorption of radio waves in the lower ionosphere. It is assumed that the mechanism for precipitation of electrons from the Earth's radiation belt is determined by the interaction of energetic electrons with VLF radio waves, which are generated due to the interaction of the amplitude-unmodulated O-mode pump wave with the ionospheric plasma near the wave reflection height.

1. INTRODUCTION

Modification of the ionospheric F_2 region by high-power HF O-mode radio waves leads to the development of various nonlinear phenomena and plasma instabilities therein. This causes the generation of a high-frequency plasma turbulence (high-frequency plasma oscillations and waves at frequencies close to the frequency of the pump wave (PW)) and a low-frequency plasma turbulence (low-frequency plasma oscillations and waves, as well as plasma-density and plasma-temperature disturbances) near the reflection height of the high-power radio wave. As a result, strong heating of the plasma, electron acceleration to suprathermal energies, electric field and current generation, plasma profile variations, modification of the ionosphere–magnetosphere coupling, and other phenomena are observed in this region.

Over the past almost 50 years of studies of the ionosphere modification by high-power HF radio waves, the main properties of artificial plasma disturbances, including their generation both in the central part of the disturbed ionospheric region, the position of which is determined by the radiation pattern of the PW and the height of its reflection, and far beyond have been explored both theoretically and experimentally. It was found that artificial plasma disturbances are recorded throughout the entire height of the ionosphere and are detected at a distance of up to thousands of kilometers from the heater in the horizontal direction [1–6].

The first results directly confirming the possibility to stimulate the energetic electron precipitations in the midlatitude ionosphere were obtained at the Sura facility in the experiment of May 12, 2008, in which

* frolov@nirfi.unn.ru

¹ N. I. Lobachevsky State University of Nizhny Novgorod, Nizhny Novgorod; ² Kazan (Volga) Federal University, Kazan, Russia; ³ CETP/IPSL, Saint-Maur; ⁴ LPSE/CNRS, Orleans, France. Translated from *Izvestiya Vysshikh Uchebnykh Zavedenii, Radiofizika*, Vol. 62, No. 9, pp. 641–663, September 2019. Original article submitted March 26, 2019; accepted September 30, 2019.

it was found that the formation of a duct at the altitudes of the outer ionosphere ($h \approx 660$ km) led to a severalfold enhancement of the flux of energetic electrons with energies $E \approx 100$ keV inside the duct. Based on these results, it was concluded in [7] that the observed electron precipitations are due to controlled excitation of the magnetospheric maser by using high-power radio waves from a ground-based short-wave transmitter to form an artificial waveguide channel—a duct with increased plasma density [5, 8, 9]. The subsequent analysis of the whole volume of collected experimental data obtained during the DEMETER mission showed the presence of precipitations in many other cases, as well, which stimulated a more detailed study of the nature of the phenomena observed.

It is well known that precipitations of energetic electrons with energies $E \leq 100$ keV into the Earth's atmosphere should cause its additional ionization at altitudes of 70–130 km (at the altitudes of the ionospheric D and E regions) [6, 10]. The additional ionization process is well studied in the case of natural events associated with the solar activity. This process leads to an increase in the plasma density at the altitudes of the lower ionosphere and additional (sometimes considerable) absorption of ultralong to short radio waves in it. In the heating experiments, the existence of such an additional ionization was detected in [11] using the Kharkov incoherent scatter radar located 960 km south–west of the Sura facility. It was found that the strongest increase in electron density above Kharkov, which reached 60–70%, was observed at altitudes of about 100 km and was absent at altitudes of about 140 km. Note that plasma disturbances could not be detected by the radar at altitudes below 90 for technical reasons. The delay time of the density disturbance appearance was about 10 min, and they were still observed 10–20 min after the pump wave switch-off. This phenomenon was explained by precipitations of energetic electrons with $E \approx 100$ keV from the Earth's radiation belts, which were stimulated by the Sura heating. According to the estimates made in [11], the flux density of such electrons should amount to 10^8 – 10^{10} m⁻²s⁻¹. These experiments directly showed that the energetic electron precipitation region affected by the Sura radiation is detected at considerable (of the order of 1000 km) distances from it, greatly exceeding the sizes of the ionospheric region exposed to a beam of high-power radio waves. According to [12], such precipitations were detected only in cases where the Earth's radiation belt was filled up with energetic electrons due to the rise in solar activity and were not detected if such an activity was absent for a long time.

Experiments on stimulation of energetic electron precipitations were repeatedly carried out at the EISCAT heater (Northern Norway) [13], which is located at more northern latitudes than the Sura facility, in areas with a high level of natural auroral activity. The latter circumstance certainly has a strong impact on the pump wave—plasma interaction process and determines the specifics of the existing ionosphere–magnetosphere coupling.

A large series of studies on stimulation of high-energy electron precipitations was performed in the HAARP heater experiments (Alaska, USA) [14], in which amplitude-modulated high-power radio waves with modulation frequencies from a few kilohertz to 10–20 kHz lying in the whistler-mode (very low-frequency, VLF) range were used for the ionosphere modification. Interacting with energetic electrons of the Earth's radiation belts, the very low-frequency waves generated in the ionosphere as a result of the nonlinear demodulation of the high-power radio wave are able to change the pitch-angle distribution of the electrons trapped in them, leading to their precipitations into the lower layers of the Earth's atmosphere.

This paper presents the results of experimental studies on stimulation of energetic electron precipitations from the Earth's radiation belt during modification of the midlatitude ionosphere by high-power HF O-mode radio waves radiated by the Sura facility. These studies are based on the Sura—DEMETER mission experiments in 2005–2010. We note that in the data concerning the properties of the energetic electron precipitations, which were presented in [9], attention is given only to sessions in which the formation of plasma ducts was detected. Today, the limitations of this approach are obvious.

2. THE MEASUREMENT ORGANIZATION

The experiments on creation of artificial plasma disturbances in the Earth's ionosphere used high-power HF O-mode radio waves that effectively interact with the plasma of the ionospheric F_2 region [3–

5]. The Sura facility described in [15] was usually switched on for 15 min, 13 min before the satellite flight through the perturbed magnetic flux tube resting on the region with strongly developed turbulence generated near the pump-wave reflection height. In a favorable ionospheric environment, such a heating duration is sufficient for the development of plasma disturbances to an almost stationary level, not only in the pump-wave reflection region, but also at the altitudes of the outer ionosphere [3, 9]. In most cases, the radiating antenna beam was tilted southward by 12° to increase the generation efficiency of artificial turbulence due to the magnetic zenith effect [4, 5]. Within the Sura—DEMETER mission in 2005–2010 there was a total of about 100 heating sessions of the ionospheric plasma with the purpose of modifying its F_2 region. The measurements were mainly conducted from March to September in a quiet or very quiet geomagnetic environment in the years of the prolonged solar activity minimum. The satellite equipment has not detected any noticeable artificial plasma disturbances during the heater operation in the daytime, which is due to the strong absorption of high-power radio waves in the lower ionosphere, the formation of a defocusing lens at altitudes of 130–180 km [16], and low (no greater than 200 km) reflection height of the PW, as well as in the case where the frequency of the high-power radio wave exceeded the cutoff frequency f_{0F_2} of the ionospheric F_2 layer (transmission heating) or when the satellite orbit passed at a distance greater than 100 km from the center of the perturbed magnetic flux tube [9].

The Sura facility (Radiophysical Research Institute of the N. I. Lobachevsky State University, Nizhny Novgorod, Russia; coordinates 56.15° N and 46.1° E, McIlwain parameter $L \approx 2.6$) is located 120 km east of Nizhny Novgorod [15]. In the range of the PW frequencies that are most frequently used in the measurements, the maximum effective radiated power of the facility with all of its three units operated synchronously is about 80 MW at the PW frequency $f_0 \approx 4300$ kHz and increases with increasing f_0 by up to about 180 MW at $f_0 \approx 6800$ kHz. The shell with $L \approx 2.6$ falls into the slot between inner and outer Earth's radiation belts. Therefore, the properties of the energetic electron precipitations at the altitude of the Sura facility strongly depend on the level of solar activity, with the increase in which the slot between the belts is filled up with energetic electrons.

French spacecraft DEMETER was launched in 2004 into a circular Sun-synchronous polar orbit with an inclination of 98.3° and an altitude of about 660 km. The satellite passed above the Sura facility at 18:00–18:30 UT in the late evening (pre-midnight) hours and at about 07:30–08:00 UT in the daytime conditions. It was equipped with a wide range of various tools and was almost perfect for detecting plasma disturbances excited in the ionosphere upon its modification by high-power HF radio waves. Energetic electrons were detected using an IDP spectrometer, which measured the energy and flux of energetic electrons in the range from 70 keV to 2.5 MeV every second in the “burst mode” regime [17]. A feature of the placement of this instrument on the casing of the satellite was that it measured the electron fluxes oriented in a direction close to orthogonal with respect to the plane of its orbit (with pitch angles lying in the range $90^\circ \pm 16^\circ$ with respect to the direction of the geomagnetic field, which corresponded to the detection of electrons trapped in the magnetic flux tube) and did not record the electrons moving in a direction close to the direction of the geomagnetic field. However, due to the low satellite altitude (about 660 km), the pitch angle for such electrons in the equatorial region of the perturbed magnetic flux tube exceeded only slightly (by a few degrees) the loss cone angle, which provided conditions for putting most of these particles into the loss cone in their interaction with VLF waves.

The work with obtained experimental data included

- 1) determining the spectral characteristics of natural precipitations of energetic electrons in different geophysical conditions when the Sura facility was out of operation to elaborate the criteria for detection of artificial precipitations against their background;
- 2) determining the properties of artificial precipitations of energetic electrons in the presence of plasma ducts formed by the ionosphere modification;
- 3) determining the properties of artificial precipitations when the ducts were not detected by the satellite tools for different reasons.

The data on conditions for all the measurement sessions considered in this paper are given in Table 1.

The second column includes the time T^* when the distance between the satellite orbit and the center of the perturbed magnetic flux tube was at a minimum and equal to D^* , time interval T_{pump} of the Sura radiation, frequency and power of the pump wave, and tilt angle of the radiation pattern of the beam of high-power radio waves. Information on ionospheric conditions, the height h_{refl} of reflection of the pump wave, the presence of artificial F_{spread} , recording of a duct with the plasma density increased by δN , and the presence of a sporadic E layer in the ionograms is included in the third column of the table. To characterize the geomagnetic activity level during measurements, the table in its third column gives the values of the ΣK_p indices (K_p is the planetary three-hour geomagnetic activity index, ΣK_p is its total daily value), and AE (AE is the auroral electrojet index). It is also indicated how much time passed from the start of the last geomagnetic disturbances to the measurement session considered, which can characterize the degree of filling of the Earth's radiation belt, including the shell with $L \approx 2.6$, by energetic electrons. We note that during the measurements analyzed in this paper, there were only weak magnetic storms (the magnetic storm strength index G did not exceed 2). We used the Universal Time UT, which for the measurement period was related to the Moscow summer time as $\text{UT} = \text{MSK} - 4 \text{ h}$.

3. ANALYSIS OF EXPERIMENTAL DATA

3.1. Recording of energetic electron precipitations in natural conditions

To analyze the properties of the precipitations observed in natural conditions, in addition to the measurement sessions given in Table 1, we chose the sessions performed in May, August, and September 2005 and 2006, and in May and June 2008, as well as individual sessions in 2010, when the DEMETER spacecraft passed above the Sura facility, which did not work either for technical reasons or because of the low cutoff frequencies, or because of the too large distance D^* between the satellite orbit and the center of the magnetic flux tube perturbed by the heating. To obtain the required information, we used the measurement results obtained from the IDP spectrometer and Langmuir probe installed onboard the satellite.

During the experimental data processing, we analyzed a) the latitude of the southern boundary of the region of strong auroral precipitations at the longitude of the Sura facility, b) the latitude of the southern edge of the region where electron fluxes were still detected, although they had a low intensity (we will attribute this part of the precipitations to their midlatitude low-intensity component), and c) the relationship of the characteristics of precipitations with the geomagnetic activity index K_p (or its daily value ΣK_p) and AE, as well as with the phase of the geomagnetic disturbance development. The results of such an analysis were used to elaborate criteria that permit one to identify the energetic electron precipitations stimulated by the ionosphere modification by high-power HF radio waves from the Sura facility against the background of their natural component.

The studies performed led to the following conclusions.

1) During the auroral activity of a low level (with $K_p \leq 2$ for a few days prior to the measurements; in the measurement day, the AE index did not exceed 100–200 nT) the southern boundary of intense precipitations at the longitude of the Sura facility for the time $T \approx 18 : 00 \text{ UT}$ does not descend below the geographic latitude $62\text{--}65^\circ \text{ N}$. On the south of this region, precipitations were either absent at all or had a low intensity with the electron energy $E \approx 100 \text{ keV}$ in them for the flux $F \leq 10 \text{ s}^{-1} \text{ cm}^{-2} \text{ ster}^{-1} \text{ keV}^{-1}$ (in what follows, we write the flux in a short form as $F \leq 10$, omitting its units). Thus, the latitude of the boundary with strong natural precipitations at a low level of auroral activity is almost 10° north of the latitude of the center of the ionosphere-heated perturbed magnetic flux tube at the altitude of the satellite orbit (660 km), which is equal to $\Phi_{\text{mft}}^* = 54.6^\circ \text{ N}$ for the southward tilt of the heater beam by an angle of 12° , which is used in most measurements, and the PW reflection height $h_{\text{refl}} \approx 230\text{--}250 \text{ km}$.

2) As the values of the AE index are increased, the southern boundary of the region with strong natural precipitations shifts to the more southern latitudes, so that at $\text{AE} \approx 300\text{--}800 \text{ nT}$ it can already reach the latitude $\Phi_{\text{mft}}^* \approx 54.6^\circ \text{ N}$, descending to the latitudes $46^\circ\text{--}52^\circ \text{ N}$ for $\text{AE} = 800\text{--}1200 \text{ nT}$. It is noted that the rate of decay of the latitude Φ_{mft}^* from AE can vary quite a lot between measurement cycles.

TABLE 1.

No.	Date. Time T^* (UT), heating time T_{pump} , distance D^* . PW frequency f_0 , PW power, tilt of radiation pattern	f_{0F_2} , h_{refl} , ΣK_p , AE. Date of the last strong geomagnetic disturbance and the maximum value of K_p for it. Generation of F_{spread} during heating. Duct recording
1	April 30, 2005 $T^* = 18:25:36$, $T_{\text{pump}} = 18:15-18:30$, $D^* = 26$ km. 4600 kHz, 100 MW, 12° southward	5.2 MHz, 287 km, $\Sigma K_p = 30^-$, AE = 400 nT. Disturbances of April 29 with $K_p = 4$. Generation of a very strong F_{spread} . Duct with $\delta N = 33\%$
2	May 25, 2005 $T^* = 18:19:54$, $T_{\text{pump}} = 18:09-18:34$, $D^* = 67$ km. 5828 kHz, 150 MW, 0°	6.6 MHz, 246 km, $\Sigma K_p = 7$, AE ≤ 25 nT. Disturbances of May 20 with $K_p = 5$. Generation of a small F_{spread} . The duct is not detected
3	August 22, 2005 $T^* = 18:14:07$, $T_{\text{pump}} = 18:11-18:19$ (before this from 15:00 in the [5 min on — 10 min off] regime), $D^* = 200$ km. 4300 kHz, 50 MW, 12° southward	5.3 MHz, 245 km, $\Sigma K_p = 17$, AE ≈ 50 nT. Disturbances of August 16 with $K_p = 4$. Generation of a strong F_{spread} . The duct is not detected
4	May 17, 2006 $T^* = 18:28:34$, $T_{\text{pump}} = 18:18-18:33$, $D^* = 39$ km. 4785 kHz, 120 MW, 12° southward	5.9 MHz, 220 km, $\Sigma K_p = 10$, AE = 320 nT. Disturbances of May 11 with $K_p = 4$. Generation of a strong F_{spread} . Duct with $\delta N = 27\%$
5	May 20, 2006 $T^* = 18:22:31$, $T_{\text{pump}} = 18:12-18:27$, $D^* = 68$ km. 5455 kHz, 150 MW, 12° southward	5.7 MHz, 225 km, $\Sigma K_p = 12^-$, AE = 70 nT. Disturbances of May 18 with $K_p = 4$. – (no ionograms). The duct is not detected
6	August 24, 2006 $T^* = 18:22:26$, $T_{\text{pump}} = 18:12-18:27$, $D^* = 55$ km. 4300 kHz, 80 MW, 12° southward	4.5 MHz, 245 km, $\Sigma K_p = 9$, AE ≤ 230 nT. Disturbances of August 19 with $K_p = 6$. Generation of a strong F_{spread} . The duct is not detected
7	April 5, 2007 $T^* = 18:22:30$, $T_{\text{pump}} = 18:12-18:27$, $D^* = 43$ km. 5480 kHz, 150 MW, 12° southward	5.5 MHz, –, $\Sigma K_p = 7$, AE = 100 nT. Disturbances of April 1 with $K_p = 4$. – (no ionograms). The duct is not detected
8	May 7, 2007 $T^* = 18:22:38$, $T_{\text{pump}} = 18:16-18:26$, $D^* = 34$ km. 4785 kHz, 120 MW, 12° southward	≤ 4.8 MHz, 270 km, $\Sigma K_p = 21^+$, AE = 270 nT. Disturbances of April 28 with $K_p = 4$. Generation of a strong F_{spread} . The duct is not detected
9	August 24, 2007 $T^* = 18:29:42$, $T_{\text{pump}} = 18:19-18:34$, $D^* = 125$ km. 4300 kHz, 80 MW, 12° southward	4.7 MHz, 240 km, $\Sigma K_p = 2$, AE = 35 nT. Disturbance of August 7 with $K_p = 4$. Generation of a strong F_{spread} . The duct is not detected
10	August 30, 2007 $T^* = 18:17:41$, $T_{\text{pump}} = 18:13-18:28$, $D^* = 64$ km. 4300 kHz, 80 MW, 12° southward	4.3 MHz, –, $\Sigma K_p = 7$, AE ≤ 35 nT. Disturbances of August 7 with $K_p = 4$. – (no ionograms). The duct is not detected
11	May 12, 2008 $T^* = 18:16:28$, $T_{\text{pump}} = 18:05-18:20$, $D^* = 21$ km. 4300 kHz, 80 MW, 12° southward	5.0 MHz, 220 km, $\Sigma K_p = 6^-$, AE ≤ 35 nT. Disturbances of April 23 with $K_p = 4$. Generation of a strong F_{spread} . $\delta N = 32\%$
12	May 28, 2008 $T^* = 18:16:28$, $T_{\text{pump}} = 18:00-18:21$, $D^* = 40$ km. 4300 kHz, 80 MW, 12° southward	4.7 MHz, 240 km, $\Sigma K_p = 19$, AE ≈ 170 nT. Disturbances of April 23 with $K_p = 4$. Very strong F_{spread} . Duct with $\delta N = 14\%$
13	August 27, 2009 $T^* = 18:03:47$, $T_{\text{pump}} = 17:53-18:08$, $D^* = 39$ km. 4300 kHz, 40 MW, 0°	4.6 \rightarrow 4.2 MHz, 240 km, $\Sigma K_p = 19$, AE ≈ 300 nT. The whole August is quiet. Generation of a strong F_{spread} . Duct with $\delta N = 20\%$

14	April 18, 2010 $T^* = 17:54:03$, $T_{\text{pump}} = 17:15-17:55$, $D^* = 25$ km. 4300 kHz, 40 MW, 12° southward	4.7 MHz, 290 km, $\Sigma K_p = 5^-$, $AE \leq 35$ nT. Disturbances of April 5 with $K_p = 5$. Generation of a strong F_{spread} . Two ducts with $\delta N = 24\%$ and 4%
15	April 28, 2010 $T^* = 18:01:13$, $T_{\text{pump}} = 17:15-17:55$, $D^* = 105$ km. 4300 kHz, 50 MW, 12° southward	5.7 MHz, 225 km, $\Sigma K_p = 6^+$, $AE \leq 35$ nT. Disturbances of April 5 with $K_p = 5$. Generation of a medium F_{spread} . The dust is not detected
16	May 14, 2010 $T^* = 17:53:13$, $T_{\text{pump}} = 17:40-17:53$, $D^* = 28$ km. 4785 kHz, 90 MW, 12° southward	6.2 MHz, 235 km, $\Sigma K_p = 5^-$, $AE \leq 35$ nT. Disturbances of May 2 with $K_p = 6$. Generation of a weak F_{spread} . $\delta N = 14\%$
17	May 27, 2010 $T^* = 17:52:42$, $T_{\text{pump}} = 17:35-17:50$, $D^* = 27$ km. 4785 kHz, 70 MW, 12° southward	5.3 MHz, 250 km, $\Sigma K_p = 4$, $AE \leq 35$ nT. Disturbances of May 2 with $K_p = 6$. Generation of a strong F_{spread} . Duct with $\delta N = 10\%$
18	June 19, 2010 $T^* = 17:58:56$, $T_{\text{pump}} = 17:39-17:59$, $D^* = 95$ km. 4300 kHz, 40 MW, 12° southward	5.1 MHz, 250 km, $\Sigma K_p = 5^+$, $AE \leq 35$ nT. Disturbances of May 29 with $K_p = 4$. Generation of a strong F_{spread} . E_{spor} from 2.0 to 5.5 MHz, non-transparent before 4.0 MHz. The duct is not detected
19	June 22, 2010 $T^* = 17:51:15$, $T_{\text{pump}} = 17:31-17:51$, $D^* = 37$ km. 4785 kHz, 40 MW, 12° southward (heating in the meandre regime with $F = 14.54$ kHz)	5.6 MHz, 245 km, $\Sigma K_p = 9$, $AE \approx 80$ nT (end of a 4-h disturbance with AE of up to 250). Disturbances of May 29 with $K_p = 4$. Generation of a strong F_{spread} . E_{spor} from 2.0 to 5.5 MHz, non-transparent before 4.0 MHz. The dust is not detected.
20	September 18, 2010 $T^* = 17:51:44$, $T_{\text{pump}} = 16:20-17:52$, $D^* = 27$ km. 4300 kHz, 50 MW, 12° southward	3.7–3.9 MHz, 235 km, $\Sigma K_p = 8^+$, $AE \approx 150$ nT. Disturbances of August 24 with $K_p = 4$. No F_{spread} in the ionograms. Duct with $\delta N = 10\%$
21	September 21, 2010 $T^* = 17:43:59$, $T_{\text{pump}} = 17:19-17:45$, $D^* = 105$ km. 4740 kHz, 105 MW, 12° southward	5.2 MHz, 225 km, $\Sigma K_p = 8$, $AE \leq 35$ nT. Disturbances of August 24 with $K_p = 4$. Generation of a very strong F_{spread} . The duct is not detected

Herein, the position of the southern boundary of the precipitation areas is to a greater extent controlled by the mean value of the AE index measured for a few hours before the experiments, rather than by its current value directly during measurements when the DEMETER spacecraft crossed the perturbed magnetic flux tube.

3) The AE index has the maximum values at the stage of a decay of geomagnetic disturbances, one or two days after the maximum values of K_p relating to their development phase were recorded. This conclusion is consistent with the results of other studies.

4) The measurement results have shown that weak electron precipitations south of the boundary of the strong auroral activity area (we denote it as the region of the “low-latitude” component of natural precipitations), if they are detected here, usually occupy a latitude band $\Phi = 50^\circ-62^\circ$ N for $AE \leq 500$ nT, irrespective of the AE value. This component of precipitations for the electron energies $E \approx 100-150$ keV is characterized by the $F \leq 10$ fluxes, and the F value for it generally depends only weakly on the latitude. Sometimes, such precipitations were observed as local structures having a length of $3^\circ-5^\circ$ in the latitude band $46^\circ-54^\circ$ N. From the foregoing, it is clear that the “low-latitude” component of weak precipitations can be detected at the altitude of the Sura facility even with a low level of geomagnetic activity. However, if there were no geomagnetic disturbances during the previous 10–15 days or more, then the energetic electron precipitations, as a rule, were not detected. The data presented demonstrate how the slot between the inner and outer Earth’s radiation belts is filled up with energetic electrons and then is emptied. As an example

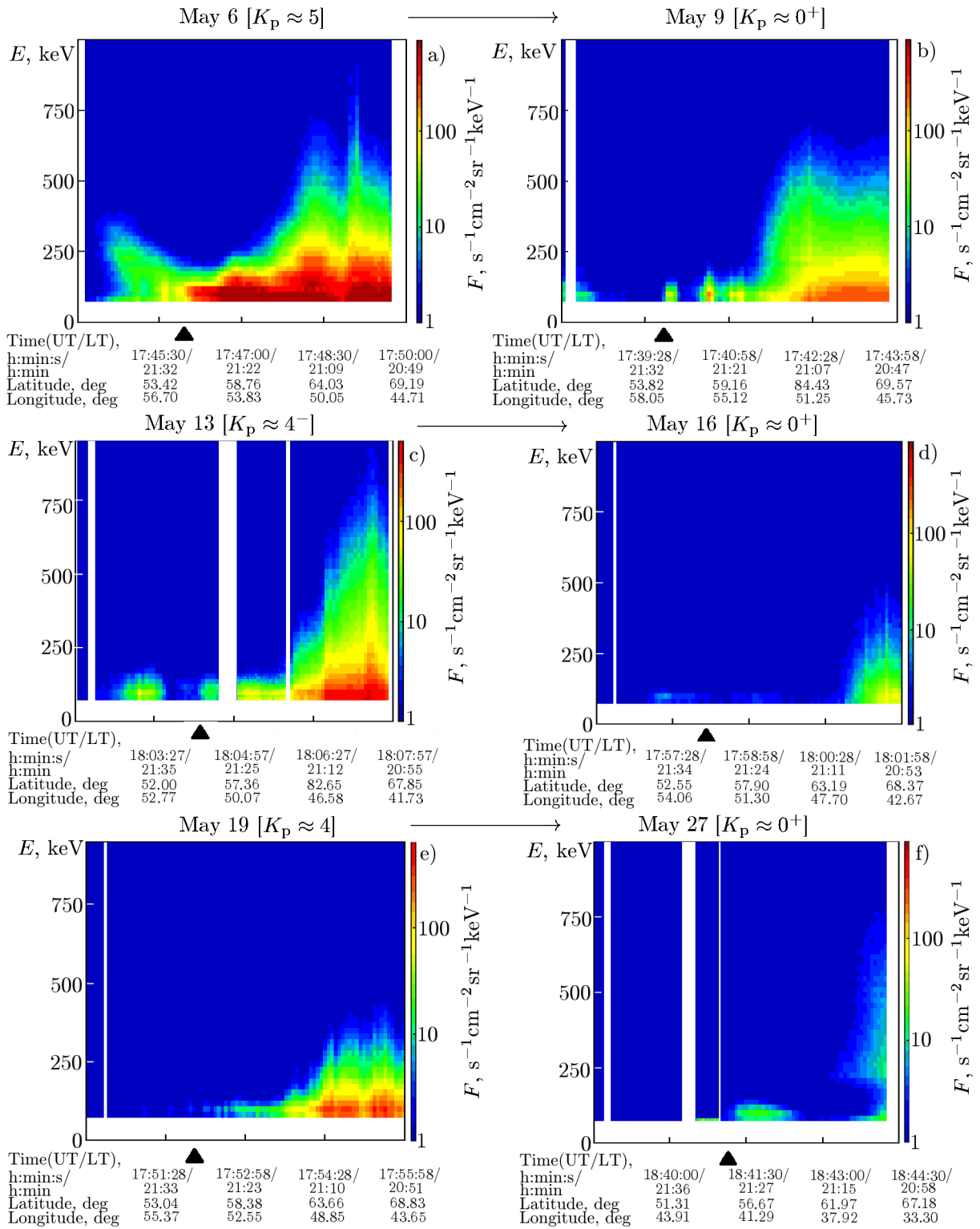


Fig. 1. Spectral and spatial characteristics of the natural precipitations of energetic electrons measured on May 6–27, 2006 under conditions of a strongly varying geomagnetic activity level day by day when the DEMETER spacecraft passed above an idle Sura facility. Hereafter, the coordinates of the center of the perturbed magnetic flux tube are marked by a black triangle under the abscissa axis.

(see Fig. 1), we consider the characteristics of energetic electron precipitations obtained in the measurements of May 6–27, 2006 under conditions of a strongly varying level of geomagnetic activity day by day, when

the DEMETER spacecraft passed above an idle Sura facility. Hereafter, the coordinate of the center of the perturbed magnetic flux tube on the panels is marked with a black triangle under the abscissa axis.

Geomagnetic disturbances with K_p equal up to 5 started on May 4. On May 5, 6, and 7 they stayed at the same high level. During May 6, the K_p value decreased from 3^- to 1^- ; on May 10, it was already within 0–1. In this cycle, the highest values of the index $AE = 300\text{--}500$ nT were recorded on May 6 (see Fig. 1a), when the intense precipitation region reached the latitude 54.6° N, but the boundary of the weaker precipitations was still 6° southward. On May 9 (see Fig. 1b) at the stage of the geomagnetic disturbance decay the K_p index already fell to 0–1 and the AE index, to 50 nT. Nevertheless, the satellite instruments continued recording individual spikes of weak precipitations at the latitude Φ_{mft}^* .

From May 10 to 11, a new spike of geomagnetic activity with K_p equal up to 4 and $AE \approx 300\text{--}500$ nT was detected. By May 15, the K_p index decreased to 1^- and the AE index, to 50 nT. On May 13, (see Fig. 1c), intense auroral precipitations were observed again, but only their “low-latitude” component was detected at the latitude of the Sura facility. An additional local precipitation region can also be seen here at the latitudes $49^\circ\text{--}52^\circ$ N. By May 16 (see Fig. 1d), the environment became quiet and the auroral activity had a low intensity. Herein, only very weak precipitations with a peak intensity at a latitude of about 51.5° N were detected at the latitude Φ_{mft}^* .

A geomagnetic activity spike with K_p equal up to 4 was observed on May 18 for a month. Measurements of May 19 (see Fig. 1e) were performed under conditions $K_p \approx 2$ and $AE \approx 150$ nT, where, judging by the K_p values, the disturbance peak was already passed. However, the auroral precipitation level was high and its “low-latitude” component descended to the Sura latitude. After May 22, the disturbance level decreased gradually, and by May 27 (see Fig. 1e) the K_p value was 0^+ at $AE \approx 50$ nT. The auroral activity was already weak and was observed only at latitudes north of 64° N in the presence of a local enhancement of precipitations in the latitude range $55^\circ\text{--}60^\circ$ N, which was located only slightly north of Φ_{mft}^* .

Thus, the results presented above show that in the measurement day the level of natural precipitations of energetic electrons is to a greater extent determined by the value of the AE index, rather than by K_p and that for sufficiently strong disturbances with $AE \geq 300\text{--}500$ nT, high-intensity precipitations can be recorded at up to the Sura latitude. The latter often comprise a “low-latitude” component of fairly weak intensity, the southern boundary of which can descend to the latitude of the heater or even slightly south of it and which does not have a strong latitude dependence of the precipitating electron flux. Similar conclusions concerning the properties of the energetic electron precipitations can be found in, e. g., [18, 19], from which it also follows that the fluxes of particles with energies 20–45 keV can exceed by a factor of 3–5 the electron fluxes with energies 85–120 keV and, therefore, put about the same energy as more energetic particles into the ionosphere.

3.2. Detection of energetic electron precipitations under conditions of the ionosphere heating by high-power radio waves

Taking into account the results of studying the properties of the natural precipitations of energetic electrons, we will analyze the observations when experiments on the ionospheric F_2 region modification were carried out at the Sura facility. Available experimental data for the convenience of their presentation and analysis were divided into four categories: 1) when the satellite passed close to the center of the perturbed magnetic flux tube, but artificial precipitations were not detected, 2) when they were detected simultaneously with the plasma duct, 3) when they were detected in the absence of the plasma duct, and 4) when the satellite passed far ($D^* \geq 100$ km) from the center of the perturbed magnetic flux tube and the plasma duct, so that it could not be detected even if it was excited. For all the measurement sessions considered here, Table 1 provides information on the Sura operation (second column) and measurement conditions (third column). These data will not be reproduced in the analysis given below.

3.2.1. Absence of artificial precipitations of energetic electrons when the satellite passed close to the center of the perturbed magnetic flux tube

Among all the data obtained, we single out the sessions in which the precipitations which certainly could be qualified as artificial were not detected during the Sura operation. In what follows, we give a short characteristic of each session.

1) In the session of April 5, 2007 (No. 7 in Table 1), which is characterized by low levels of auroral and geomagnetic activity and was conducted four days after the start of geomagnetic disturbances, natural “low-latitude” precipitations of electrons with energy E up to 170 keV and an almost constant maximum value of the flux $F \approx 80$ for $E \approx 100$ keV were observed in the latitude range 56.2° – 61.5° N (see Fig. 2a); a region with high auroral activity was detected at the higher latitudes. A feature of this session is the ionospheric plasma heating where $f_0 \approx f_{0F_2}$. In such conditions, the excitation of intense artificial ionospheric turbulence was not observed and the plasma duct was not formed because of the high level of the PW penetration into the outer ionosphere [9]. In this and some other sessions presented below, white stripes in the figures correspond to periods in which the IDP instrument did not perform the energetic electron recording for technical reasons.

2) The ionosphere modification in the session of August 30, 2007 (No. 10) was performed for $f_0 \approx f_{0F_2}$, and only for a short time (5 min), before the satellite flyby. Such characteristics of the heating session, as in the previous case, do not correspond to the conditions of the intense artificial turbulence excitation. The session was conducted 23 days after the start of geomagnetic disturbances and is characterized by a low level of auroral and geomagnetic activity. Natural “low-latitude” precipitations of electrons with $F \approx 10$ for $E \approx 100$ keV were observed in the latitude range 57.7° – 62° N (330–820 km north of Φ_{mft}^*) with their peak intensity at the latitudes 59.5° – 60.8° N.

3) The features of the session of April 28, 2010 (No. 15; see Fig. 2b), which was conducted 23 days after the start of geomagnetic disturbances and is characterized by a low level of geomagnetic activity, were heating for f_0 at 1.4 MHz below f_{0F_2} (i. e., far from the cutoff frequency) and a moderately high (50 MW) heating power. It was shown in [9] that for smaller PW powers, the formation of a duct can no longer be detected. In the considered session, “low-latitude” precipitations of electrons with $E \leq 140$ keV were observed only at the latitudes 56.0° – 62.3° N (150–850 km north of Φ_{mft}^*) with the peak flux $F \approx 10$ for $E \approx 100$ keV at the latitudes 56.7° – 57.2° N. Two more individual strong precipitation spikes were recorded slightly south of this region. North of this region, the electron energy and the electron flux decreased gradually when approaching the latitude 62.7° N (i. e. when moving closer to the region of high auroral activity). Because of the long distance to the center of the perturbed magnetic flux tube ($D^* = 105$ km) and termination of heating 6 min before the satellite flyby, the satellite instruments could not record the duct or any other plasma disturbances. However, it cannot be excluded that in this case, the enhancement of the precipitation intensity in the latitude range 56.7° – 57.2° N could be due in part to the Sura operation. Another feature of this session is a large time between the end of geomagnetic activity and the measurements when the shell at $L \approx 2.6$ could already lose energetic electrons.

4) The features of the session of June 19, 2010 (No. 18), which was conducted 21 days after the start of geomagnetic disturbances, were a low power of the PW radiation (40 MW), a low level of geomagnetic activity, and that a sporadic E_{spor} layer that is translucent at the heater wave frequency was present during the ionosphere modification. This could lead to a considerable attenuation of the PW power transferred to the upper ionosphere. In this session (see Fig. 2c), the “low-latitude” component of precipitations of electrons with $E \approx 100$ keV were detected at the latitudes 53.3° – 61.7° N (from 140 km south to 820 km north of Φ_{mft}^*) with the peak flux $F \approx 20$ for $E \approx 100$ keV at the latitudes 56.3° – 57.7° N. South and north of the region of the maximum, the intensity and flux of precipitations smoothly decrease, and the process is faster in the south direction. A small peak of precipitation intensity takes place at the latitude $\Phi_{\text{mft}}^* = 54.6^\circ$ N. A long distance to the center of the perturbed magnetic flux tube ($D^* = 95$ km), a low PW power, and the presence of E_{spor} have been the reasons why the formation of a duct and other plasma disturbances were not detected. Based on the available data, the main part of precipitations at the latitudes

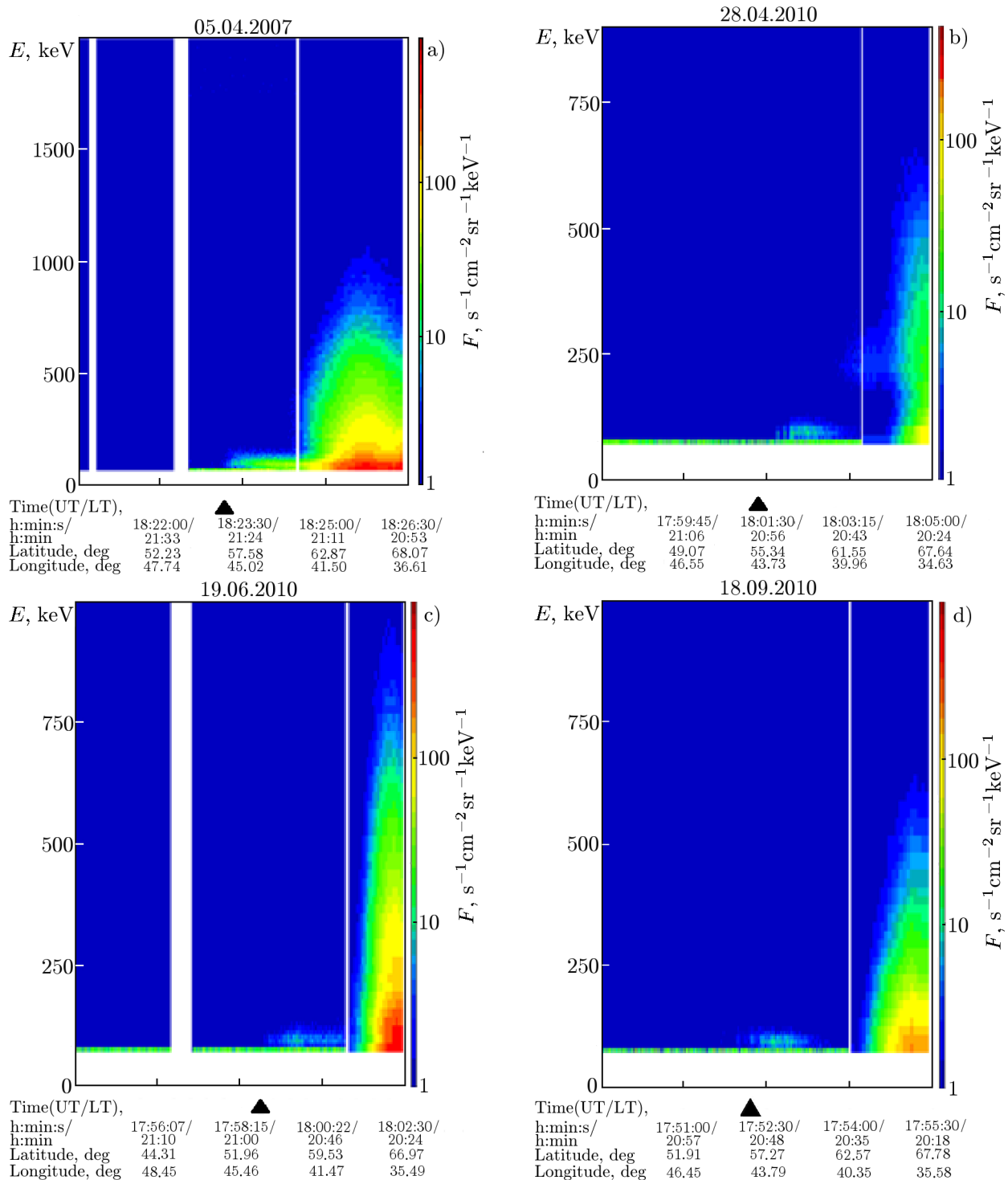


Fig. 2. Examples of the sessions in which the precipitations that could certainly be qualified as artificial (sessions 7, 15, 18, and 20 on panels a, b, c, and d, respectively) were not detected during the Sura operation.

south of the auroral activity area cannot be attributed to artificial, although it cannot be excluded that a slight enhancement of energetic electron fluxes near Φ_{mft}^* could be due to the Sura operation.

5) The session of June 22, 2010 (No. 19) was conducted 23 days after the start of geomagnetic disturbances under conditions of a low level of geomagnetic activity. The features of this session were a low power of the PW radiation (40 MW) and the presence of an almost opaque (shielding) E_{spor} layer during the

ionosphere modification, which explains the absence of the duct formation and other plasma disturbances. By characteristics, it is similar to session No. 18. In this session, the “low-latitude” precipitations of electrons with $E \approx 120$ keV were observed at the latitudes 54.3° – 61.7° N (from 30 km south to 780 km north of Φ_{mft}^*) with a pronounced maximum of the $F \approx 20$ flux for $E \approx 100$ keV at the latitudes 57.9° – 59.7° N; south and north of the region of the maximum, the electron energy and the electron flux decrease gradually (slower in the north direction). Energetic electron precipitations with apparent signatures of their artificial nature were not detected, although it is possible that the enhancement of energetic electron fluxes near Φ_{mft}^* can be due to the Sura operation.

6) The features of the session of September 18, 2010 (No. 20; see Fig. 2*d*) were a low power of the PW radiation (50 MW) and the fact that during the satellite flyby above the facility the PW frequency was already higher than the cutoff frequency f_{0F_2} , although at the start of the heating, which was switched on 1.5 h before the flyby, f_0 was lower than f_{0F_2} , which provided conditions for the creation of a plasma duct and excitation of plasma turbulence at the altitudes of the outer ionosphere. Energetic electron precipitations with apparent signatures of their artificial nature were not detected. In this session, “low-latitude” precipitations of electrons with $E \leq 120$ keV were observed at the latitudes 55.4° – 61.2° N (90–730 km north of Φ_{mft}^*) with the maximum precipitation intensity ($F \approx 10$ for $E \approx 100$ keV) at the latitudes 57.2° – 58.6° N. From this region, the precipitation intensity decreased gradually to the north and slightly faster to the south. From the analysis of this session it can be concluded that the presence itself of a plasma duct is not a sufficient condition for generation of artificial precipitations of energetic electrons, for example, due to their absence at $L \approx 2.6$.

Completing our consideration of this set of experimental data, we note once again that most of the measurement sessions discussed above were carried out a significant time later (more than 20 days) after the last geomagnetic disturbances under conditions of a low auroral activity when the AE index, with one exception, did not exceed 100 nT.

The experimental data presented above suggest that the artificial energetic electron precipitations stimulated by the ionosphere modification were not detected when the conditions for generation of intense plasma disturbances near the PW reflection height were not fulfilled. This refers to the cases of transmission heating or even heating under the conditions $f_0 \approx f_{0F_2}$ for a PW frequency by more than 1 MHz lower than f_{0F_2} , at low PW powers ($P_{\text{eff}} \leq 40$ MW), on short (a few minutes) heating times, and in the presence of a sporadic E layer that shields, partially or completely, the ionospheric F_2 region. Under the same conditions, the generation of ducts with increased plasma density at the altitudes of the outer ionosphere is not observed [3, 9]. Artificial precipitations were not detected, as well, when geomagnetic conditions before the measurements remained quiet for a long time, which can be due to the absence of energetic electrons at $L \approx 2.6$, which is between the inner and outer Earth’s radiation belts in a quiet geomagnetic environment. Nevertheless, the studies have shown that in the latitude range 56° – 59° N local (in latitude) energetic electron precipitations, which in some of their characteristics can be due to the Sura operation, are observed sometimes.

3.2.2. Energetic electron precipitations in the presence of plasma ducts of the plasma density

These sessions are interesting in that the recorded ducts with increased plasma density are obviously artificial formations created by high-power radio waves when the ionosphere is heated by high-power HF radio waves [5, 9]. In three of the nine sessions in which the formation of a duct was observed, there was their clear effect on the intensity of energetic electron precipitation. In three sessions, this effect was observed, but had a not so pronounced form, or the results of these measurements were additionally affected by technical reasons. In another three sessions, there was no notable effect of ducts on the characteristics of precipitations. Of the last three sessions, one (No. 20) was considered in the previous section.

Consider first the session in which the effect of the duct as a stimulating factor for the energetic electron precipitation was undeniable.

1) In the session of May 12, 2008 (No. 11; see Fig. 3*a*), precipitations of energetic electrons with

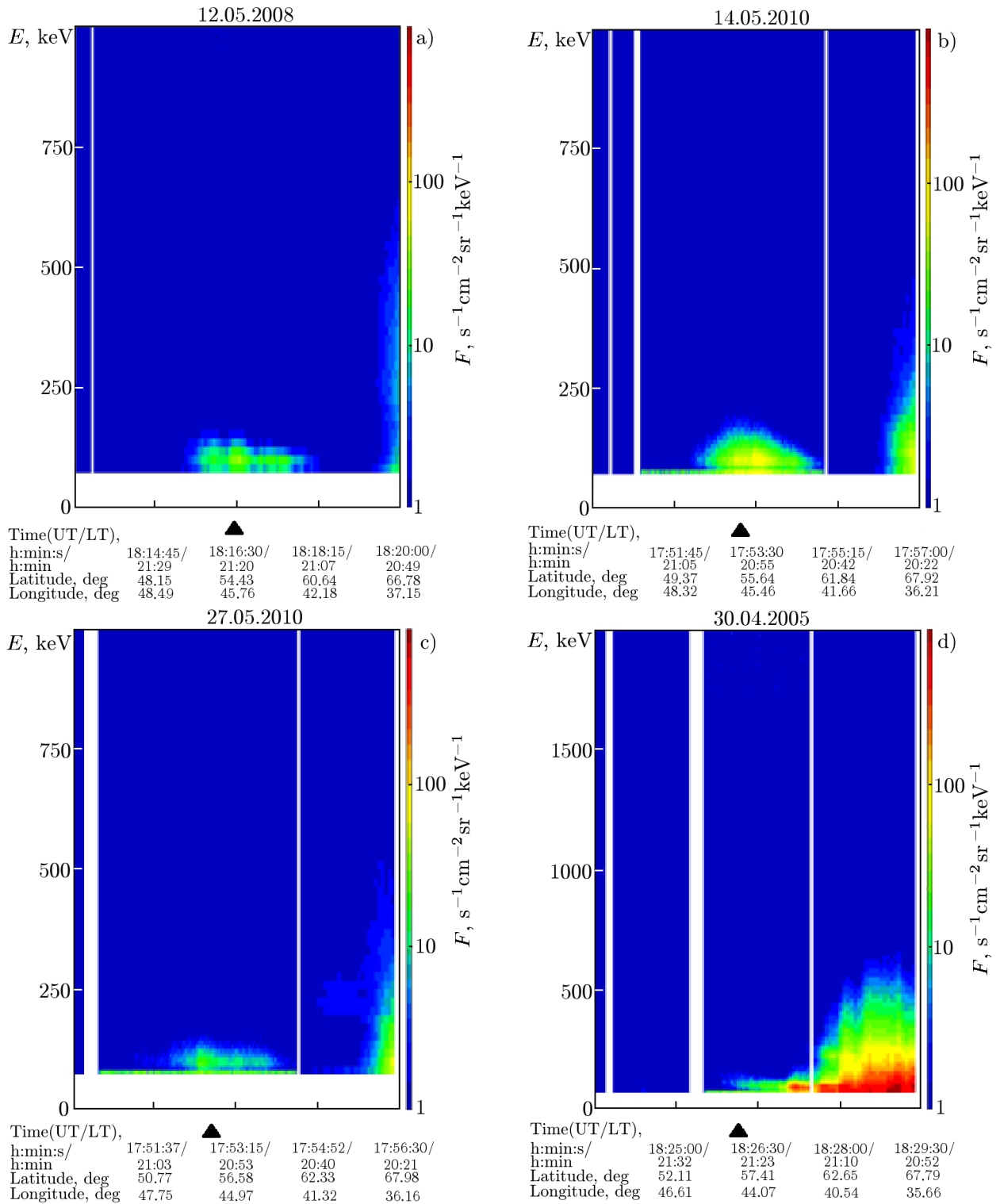


Fig. 3. Examples of the sessions in which artificial precipitations and ducts with increased plasma density were detected (sessions 11, 16, 17, and 1 on panels *a*, *b*, *c*, and *d*, respectively.)

$E = 70\text{--}150$ keV and $F \approx 5\text{--}70$ were observed in the latitude range $50.5^\circ\text{--}60.2^\circ$ N (450 south and 620 km north of Φ_{mft}^*), and the electron flux along the satellite orbit decreased with increasing distance from the satellite to the center of the perturbed magnetic flux tube. The maximum intensity of precipitations with $F \approx 70$ for $E \approx 100$ keV was detected when the satellite crossed the plasma density duct; however, 180 km

south of Φ_{mft}^* there was a local enhancement of the precipitation intensity. In that session, strong plasma disturbances were excited at a low level of auroral and geomagnetic activity, but with increased integral electron density in the ionosphere. The measurements were taken 19 days after the start of geomagnetic disturbances. Note that the measurement results in this particular session were considered in [7], where it was concluded that more intense precipitations of energetic electrons inside the duct, which were observed during the Sura radiation, are determined by the excitation of a magnetospheric maser. Based on the obtained data it became clear that not only the energetic electron precipitations inside the duct are artificial, but also precipitations south and north of the duct (only at a distance of 1070 km along the satellite orbit, almost along the meridian) were also stimulated due to the ionosphere modification by high-power HF radio waves.

2) Measurements in the session of May 14, 2010 (No. 16) were taken 12 days after the start of geomagnetic disturbances. Precipitations of energetic electrons with $E = 70\text{--}200$ keV and $F \approx 5\text{--}100$ (see Fig. 3b) were observed at the latitudes $50.3^\circ\text{--}60.7^\circ$ N (at a distance of 480 km south to 680 km north of Φ_{mft}^*); the recorded electron flux and electron energy decreased with increasing distance from the center of the perturbed magnetic flux tube. The local maximum of the precipitation intensity with $F \approx 80$ for $E \approx 100$ keV took place when the satellite crossed the plasma duct, which was detected slightly southward of Φ_{mft}^* , which can be due to the “magnetic zenith” effect, when the region with the strongest plasma disturbances turns out to be shifted by 20–30 km from the center of the radiation pattern of the beam of high-power radio waves in the magnetic zenith direction [2, 3, 5]. However, the maximum fluxes $F \approx 100$ of the electrons with $E \approx 100$ keV were observed at 80–200 km north of the center of the perturbed magnetic flux tube. The latter can be due to the higher content of energetic electrons on the L -shells located closer to the inner boundary of the external radiation belt as compared with their content at $L \approx 2.6$. Note that in the north direction the precipitation intensity decreased slower than in the south direction. These data is direct evidence that not only precipitations in the duct, but also those south and north of the duct at a distance of 1160 km along the satellite orbit were also stimulated by the ionosphere heating. These measurements were taken at a low level of auroral and geomagnetic activity 12 days after the start of disturbances, when the energetic electron content notably decreases in the slot between the radiation belts. It was found in [9] that the excitation of strong plasma disturbances in the outer ionosphere was observed in this session, which is evidence for a high efficiency of the high-power radio-wave interaction with the plasma.

3) Measurements in the session of May 27, 2010 (No. 17) were taken 25 days after the start of geomagnetic disturbances at a low level of auroral and geomagnetic activity. Artificial precipitations of energetic electrons with $E = 70\text{--}150$ keV and $F \approx 5\text{--}70$ (see Fig. 3c) were observed at the latitudes $49.5^\circ\text{--}61.0^\circ$ N (at a distance of 570 south to 710 km north of Φ_{mft}^*); the recorded electron flux and electron energy decreased with increasing distance, and the decrease was faster southward than northward. The maximum intensity of precipitations with $F \approx 40$ for $E \approx 100$ keV took place when the satellite crosses the plasma duct and slightly south of it. The duct itself was located 30 km south with respect to the calculated value of the latitude Φ_{mft}^* of the center of the flux tube, which is attributed to the “magnetic zenith” effect. As in the previous session, the excitation of strong plasma disturbances took place.

4) During the sessions of May 17, 2006 (No. 4) and May 28, 2008 (No. 12), when the satellite passed through the plasma duct, the IDP spectrometer was switched off for about 23 s, and only at the edge of this band one could see the increased level of the precipitation intensity of energetic electrons with $E \approx 100$ keV as the precipitation intensity decreased further to the north. It can be assumed that these sessions, too, confirm the impact of the PW-induced ducts with increased plasma density on the properties of the energetic electron precipitations.

We consider separately the measurement of April 30, 2005 (session No. 1; see Fig. 3d). Measurements in this session were taken in a day after the start of geomagnetic disturbances under conditions of increased auroral and geomagnetic activity. It is seen from the measured characteristics of energetic electrons that south of the auroral activity area (south of 59° N) there are two components of precipitations. The first one is characterized by the higher flux and weak dependence of the electron energy E on the latitude. The second component, with a low electron flux ($F \leq 10$), is of diffusive nature; it is characterized by a gradual

increase in electron energy to the south (with approaching Φ_{mft}^*) and an abrupt break of the spectrum at the latitude 54.5° N, at about 100 km north of Φ_{mft}^* . The first component of precipitations can be attributed to the “low-latitude” component of natural precipitations, while the second component has apparent signatures of its artificial origin. It should be concluded that one day from the start of geomagnetic disturbances is not enough to ensure that the slot between the radiation belts is filled up with energetic electrons.

Completing our consideration of the results related to this section, we note that the precipitations were not detected on August 27, 2009 (session No. 13) April 18, 2010 (session No. 14), when the conditions for stimulation of the energetic electron precipitations from the Earth’s radiation belt were favorable. Their absence, as in [12], can be due to the fact that the ionosphere was heated when the geomagnetic conditions were quiet for a long time before the measurement, and therefore the electrons with energies $E \geq 70$ keV were absent at $L \approx 2.6$. The presence of energetic electrons in the slot between the Earth’s radiation belts is an important condition for stimulating their precipitation upon modification of the midlatitude ionospheric F_2 layer by the high-power Sura radiation.

The results of the measurements permit us to formulate the signatures of the artificial nature of the energetic electron precipitations from the Earth’s radiation belt, which were observed in the Sura—DEMETER experiments during the ionosphere modification by high-power HF radio waves in the late evening and midnight hours:

1) as a rule, the maximum intensity of precipitations is observed inside the perturbed magnetic flux tube (especially when a duct with increased plasma density is formed in it);

2) in the geomagnetic meridian plane, the precipitation intensity gradually decreases north of the center of the perturbed magnetic flux tube, extending to the area of auroral latitudes, and much more sharply south of it;

3) the energy of the precipitating electrons with their maximum fluxes up to $F \approx 100$ is about 100 keV as measured in the $E \geq 70$ keV region;

4) the precipitations are observed when the effective PW radiation power transferred to the upper ionosphere exceeds 40 MW and at the same time there is effective interaction between the high-power radio wave and the plasma of the F_2 layer, which manifests itself as generation of strong F_{spread} in the vertical sounding ionograms and as anomalous attenuation of O-mode radio waves at frequencies near or above the PW frequency.

3.2.3. Precipitations in the absence of detected plasma density ducts

In this section, the results of measurements obtained in the sessions, in which the duct was not detected, plasma disturbances were weak or absent; however, the appearance of the HF-induced energetic electron precipitations was observed.

1) The measurements in the session of May 25, 2005 (No. 2; see Fig. 4a) were taken 25 days after the start of geomagnetic disturbances. The session was specific in that it was conducted at a high cutoff frequency, $f_{0F_2} \approx 6.6$ MHz, and for the vertical radiation pattern of the heater, but with a high effective PW radiation power $P_{\text{eff}} \approx 150$ MW. Herein, only a weak F_{spread} was recorded in the ionograms. The detected low level of plasma disturbances in this session can be related to the high cutoff frequencies, the vertical radiation pattern of the high-power radio wave, and a fairly long distance $D^* = 67$ km between the satellite orbit and the center of the perturbed magnetic flux tube. The duct was not detected by the satellite instruments, which can be due to both a long distance D^* and a low efficiency of the PW—plasma interaction. Despite the far-from-optimal conditions for the F_2 -region modification, intense precipitations with the maximum intensity at the latitude Φ_{mft}^* were detected in this session. Further research is needed in order to understand the reason. The results we obtained lead to the conclusion that the transverse size of the precipitation area should notably exceed 130 km. It was mentioned above that north of the latitude Φ_{mft}^* till the auroral region (at a distance of about 700 km) the precipitation intensity decreased gradually, and the decrease was faster in the south direction (at a distance of about 450 km).

2) The session of May 20, 2006 (No. 5; see Fig. 4*b*) is characterized by a weak auroral and geomagnetic activity: geomagnetic activity started to increase on May 17, and only a slight residual disturbance was recorded in the measurement day (because of the long distance $D^* = 68$ km). The most intense precipitations were observed at the latitude Φ_{mft}^* . The size of the precipitation area across the geomagnetic meridian can be estimated as exceeding 140 km. North of the latitude Φ_{mft}^* towards the auroral precipitation region (about 700 km) and at a distance of about 600 km southward the precipitation intensity decreased gradually, but the precipitation intensity itself in the southern part was much lower than in the northern part.

3) The session of May 7, 2007 (No. 8; see Fig. 4*c*) is characterized by the increased level of geomagnetic and auroral activity: geomagnetic disturbances started 9 days before the start of measurements, but on the 7th of May there was a repeated disturbance spike. The measurements were taken at $f_0 \approx f_{0F_2}$. Strong F_{spread} was excited during the heating. The duct was not detected, which is due to the long distance $D^* = 68$ km and closeness of the PW frequency to f_{0F_2} . In this session, the most intense precipitations were observed at 170–310 km north of Φ_{mft}^* . North of the latitude with the maximum level of precipitations, their intensity at a distance of about 450 km decreased gradually with approaching the auroral region, while south of Φ_{mft}^* the precipitation intensity abruptly decreased. The size of the precipitation area across the geomagnetic meridian can be estimated as exceeding 140 km. Close results were also obtained on August 24, 2006 (session No. 6).

4) The session of September 21, 2010 (No. 21; see Fig. 4*d*) is characterized by a weak auroral and geomagnetic activity; the disturbance level was low for the previous four weeks. A very strong F_{spread} was excited during the heating. The duct was not detected because of the long distance $D^* = 105$ km. Precipitations were observed only north of the latitude Φ_{mft}^* with their maximum intensity at 210 km north of Φ_{mft}^* and with a smoothly decaying intensity further to the north till the auroral precipitation region. This session is specific in that a fairly high level of artificial precipitation took place despite the weak level of geomagnetic activity for a long time before the measurements. The precipitations were recorded only north of Φ_{mft}^* . Additional research is needed to understand the reasons for such a behavior of the precipitations. Close results were also obtained on August 24, 2007 (session No. 9).

5) In the session of August 22, 2005 (No. 3) the measurements were taken 5 days after the start of geomagnetic disturbances. The minimum distance before the satellite orbit and the center of the perturbed magnetic flux tube was $D^* \approx 200$ km; therefore, the duct and the plasma disturbances were not detected by the satellite tools. Intense auroral precipitations of energetic electrons with $E > 1000$ keV were observed north of 62.5° N. The maximum precipitation intensity of energetic electrons with $E \approx 100$ keV was detected near Φ_{mft}^* . The precipitation intensity decreased gradually at a distance of about 680 km northward and faster at a distance of about 350 km southward. Note that by its characteristics, these precipitations, with allowance for the PW power, are close to the precipitations detected on May 25, 2005 (session No. 2). Based on these data, it can be concluded that across the geomagnetic field lines, precipitations can also be observed at a distance of about 200 km (and maybe even farther) from the center of the perturbed magnetic flux tube.

In the analysis of the whole volume of experimental data obtained within the Sura—DEMETER mission, the following fact should be taken into account. Measurements in which the satellite passed at the distance D^* equal to 200 km from the center of the perturbed magnetic flux tube were taken only in 2005 (at the start of work in this program). The plasma disturbances, which, as a rule, are located within a tube with a diameter of about 100 km (or at $D^* \leq 50$ km) based on a region with highly developed artificial ionospheric turbulence near the PW reflection height, are no longer detected at such distances [9]. Therefore, in the later experiments the measurements were performed only if the distance D^* was less than 75 km (seldom for $D^* \approx 100$ km). This explains the limited number of sessions held for large D^* and related inability to more accurately determine the nature of the dependence of the precipitation intensity on D^* .

Summarizing all the obtained experimental data, we can conclude that the precipitation region is stretched along the geomagnetic meridian, having longitudinal dimensions of up to 1300 km and transverse dimensions, no less than 400 km. It should also be mentioned that under conditions of long absence of

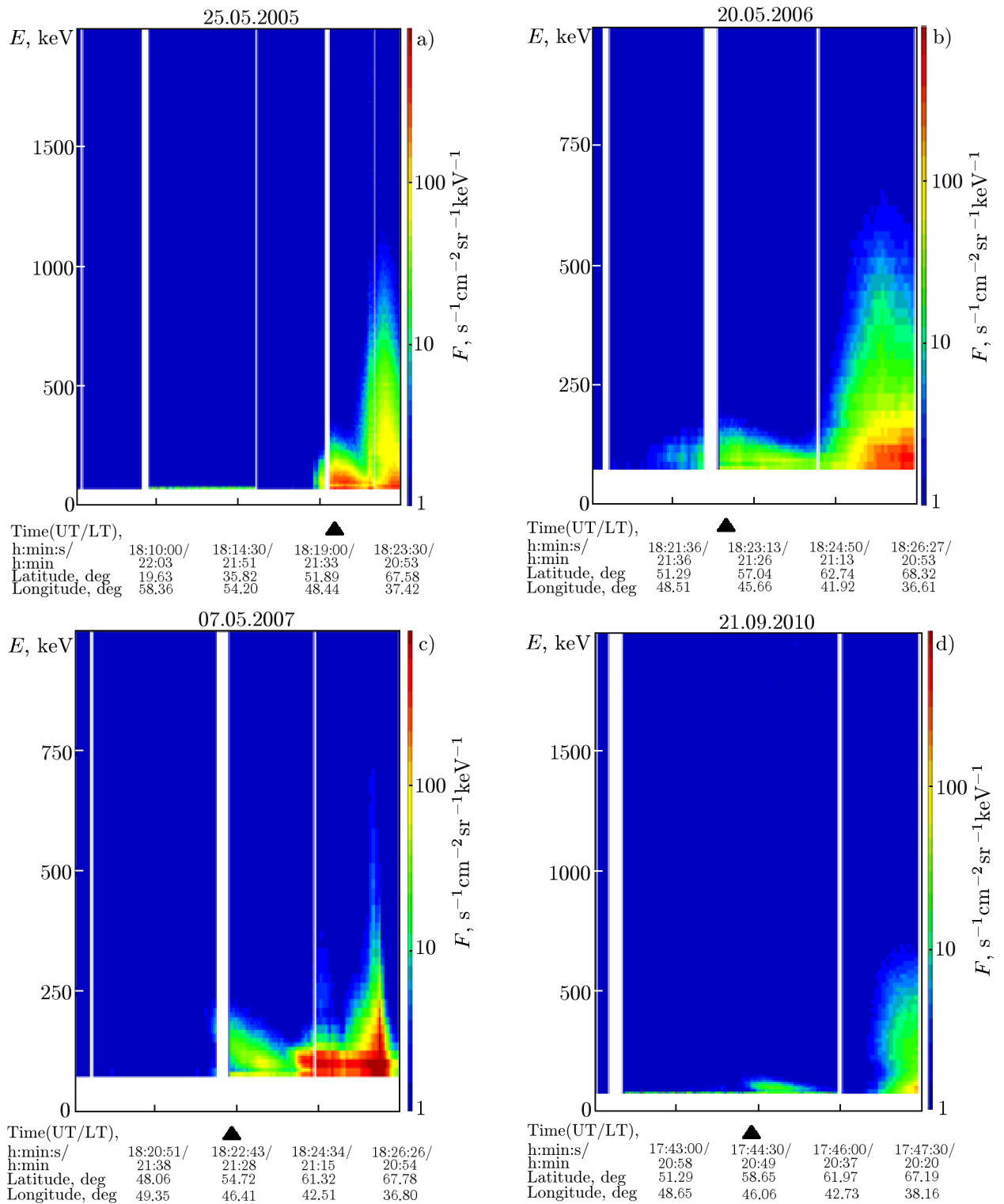


Fig. 4. Examples of the sessions where artificial precipitations were detected in the absence of ducts with increased plasma density (sessions 2, 5, 8, and 21 on panels a, b, c, and d, respectively).

geomagnetic disturbances before measurements, the maximum of the precipitation intensity can be shifted northward from Φ_{mft}^* by 200–300 km in the absence of precipitations near the latitude Φ_{mft}^* (near the Sura facility). This displacement can be due to the following reasons. Firstly, it may be caused by the higher content of energetic electrons at the higher-latitude magnetic field lines (for $L \geq 3$), when they already fall

into the outer radiation belt, in the absence of such electrons in the flux tube corresponding to $L \approx 2.6$, which is based on the region of intense interaction of a high-power radio wave with the plasma of the ionospheric F_2 region. Secondly, as was shown in [20, 21], this can also be due to the presence of areas with sufficiently intense generation of artificial ionospheric turbulence north of the area determined by the center of the radiation pattern of the beam of high-power radio waves. The latter is determined by the refraction and focusing of the beams on a region with developed artificial kilometer plasma-density inhomogeneities in the main lobe of the radiation pattern. In addition, increased generation of artificial turbulence in this direction can be supported by sufficiently intense radiation of a high-power radio wave in the first side lobe of the Sura antenna when it is tilted by 12° southward, which is commonly used in our measurements to achieve the magnetic zenith effect.

4. IONIZATION OF THE IONOSPHERIC PLASMA BY ENERGETIC ELECTRONS

The results presented in this paper clearly demonstrate that modification of the midlatitude ionosphere by high-power HF radio waves in the late evening and pre-midnight hours in certain conditions stimulates intense precipitation of electrons from the Earth's radiation belt with energies $E \approx 100$ keV and with a flux of up to $100 \text{ s}^{-1} \text{ cm}^{-2} \text{ ster}^{-1} \text{ keV}^{-1}$. Herein, the region of precipitations of these electrons has spatial dimensions of about 1300 km along the geomagnetic meridian with a larger extension north of the facility and no less than 400 km across it with the maximum precipitation intensity usually in the heater location. Such electrons are capable of causing an additional plasma ionization at the altitudes of the D and E regions ($h \approx 70$ – 130 km), which leads to an increase in absorption of radio waves at these altitudes [6, 10–12, 14, 22]. Changes in the amount of absorption are easy enough to detect in experiments and are a diagnostic signature for the occurrence of high-energy electron precipitations from the Earth's radiation belt. It is clear that, unlike the satellite measurements, the detection of this effect by using, e.g., vertical ionosphere sounding stations, provides information on conditions of the appearance and their characteristic times, which gives important information about their nature. In our case, such measurements were performed using the ionospheric station located near Kazan at a distance of 170 km east of the facility [23].

Analysis of the experimental data pertaining to the evening hours of measurements, which was performed in [23], has shown that an absorption effect of the vertical sounding signals passing through the ionospheric E region existed in the sessions of the midlatitude ionosphere heating by high-power HF O-mode radio waves from the Sura facility. A characteristic rise time of absorption (or of the appearance of energetic electrons) was 5–10 min. There was an ionosphere modification pre-history effect, where in the first heating pulse after a long pause in the heater operation, the suppression of the sounding signal intensity appears only 12 min after the PW switch-on, but it starts to develop almost immediately after its second pulse is switched on. Moreover, after the first PW pulse, the recovery of the signal intensity lasted for about 5–10 min and was only 2–4 min for its second PW pulse. From the results of this measurement session it can also be concluded that for the third and subsequent switch-on pulses of a high-power radio wave, a distinct correlation between the sounding signal intensity and the high-power wave switch-on is violated. Namely, the signal could have a low intensity or, conversely, could be the maximum both during the high-power wave radiation and in the heating pause. This indicates the existence of an accumulation effect and an aftereffect from different cycles of PW radiation, which is especially pronounced with short times of the PW radiation and pause (e.g., in the cyclic regime [5-min radiation — 5-min pause] of the heater operation. Basing on all the available data, it can be concluded that for such studies, a 15-min pause between the PW radiation pulses may appear too short to avoid the manifestation of the aftereffect and accumulation effect which strongly distort the obtained results and introduce great uncertainty in their interpretation.

A more detailed discussion of the features of the impact of the HF-stimulated energetic electron precipitations on characteristics of the lower ionosphere is beyond the scope of this work and will be presented elsewhere. Prospects for these studies are obvious. Using routine ionosonde measurements and without conducting satellite measurements, which due to the rare satellite flights in the right time close to the center of the perturbed magnetic flux tube preclude the obtaining of required information in full for a reason-

able duration of measurements, one can study the dynamic characteristics of precipitations, their diurnal dependence and dependences on geomagnetic activity, ionospheric disturbance, and the characteristics of a high-power radio wave (its power, polarization, tilt angle of the beam, PW reflection height, etc.). In addition, the already accumulated database of ionosonde measurements makes it possible to perform part of this work without conducting new large-scale heating experiments.

5. CONCLUSIONS AND FINAL REMARKS

We have studied the features of stimulation of energetic electron precipitations from the Earth's radiation belt during heating of the F_2 region of the midlatitude ionosphere by high-power HF radio waves. The experiments were conducted in 2005–2010 using the Sura facility with the energetic electrons recorded by the onboard equipment of the French spacecraft DEMETER. The signature of the artificial nature of the energetic electron precipitations were determined.

1) The maximum intensity of precipitations is usually observed inside the perturbed magnetic flux tube resting on the region of the most intense generation of artificial ionospheric turbulence and strong ionospheric plasma heating near the PW reflection height. The precipitation intensity increases in the presence of a duct with plasma density increased relative to the background value.

2) The precipitation area along the geomagnetic meridian is up to 900 km north and up to 400 km south of the heater. The size of the precipitation region in the direction orthogonal to the meridian is no less than 400 km.

3) The maximum precipitating electron flux with $F \approx 100 \text{ s}^{-1}\text{cm}^{-2}\text{ster}^{-1}\text{keV}^{-1}$ takes place for electrons with the energy $E \approx 100 \text{ keV}$.

4) Precipitations are observed when the effective PW radiation power exceeds 40 MW and the conditions of effective interaction between a high-power radio wave and the plasma of the ionospheric F_2 layer are fulfilled. The absence of precipitations after a long period of low geomagnetic activity can be due to the absence of energetic electrons at $L \approx 2.6$ located between the Earth's radiation belts and on which the Sura facility is located.

According to the experimental data obtained, the total power transferred by the precipitating electrons with energy of the order of 100 keV can be estimated as 200–600 kW, which is comparable with the high-frequency power $P \approx 500 \text{ kW}$ generated by the transmitters of the heating facility. Actually, the power transferred by the precipitating electrons can be severalfold greater if the energy of electrons with $\leq 70 \text{ keV}$ [18, 19], as well as the precipitations also observed in the ionosphere that is magnetically conjugate to the Sura facility, are taken into account [24].

The considered results on stimulation of energetic electron precipitations from the Earth's radiation belt and their effect on the lower ionosphere permit an interpretation of the hitherto unexplained effect discovered in the first experiments at the facility in Platteville (Colorado, USA) when measuring the heating-stimulated absorption of radio waves in the ionospheric D region, which is described in [25]. It was shown in that paper that after a long (10-min) heating of the ionosphere by high-power radio waves there was relaxation of absorption of the probing radio waves, which was never detected with short (40-ms) PW radiation pulses for which the characteristic rise time and attenuation of absorption were certainly less than 40 ms. In addition, the ionosphere heating by high-power O-mode radio waves was more efficient compared to X-mode waves. Both results did not fit into the framework of the ideas accepted at that time about modification of the lower ionosphere by high-power radio waves. It is clear now that the observed effects were related with HF-stimulated energetic electron precipitations whose impact on the lower ionosphere lasts 10–15 min and that for stimulation of precipitations, the ionospheric plasma modification by high-power O-mode radio waves is much more efficient due to the resonant nature of the PW — plasma interaction.

As is known, an effective mechanism for stimulation of energetic electron precipitations from the Earth's radiation belts is their interaction with VLF radio waves (whistler mode) [14, 26]. For this, either direct emission of these waves by ground-based VLF transmitters or their generation upon demodulation of the amplitude-modulated high-power HF radio wave at the ionospheric altitudes due to the Getmantsev

effect are usually employed [27]. This is especially effective in the high-latitude ionosphere due to the presence of a strong auroral electrojet.

The performed studies [28–31] showed that VLF waves can also be generated when the ionosphere is heated with the PW radiated in the carrier-frequency regime. This is due to the excitation of lower-hybrid waves during the development of a thermal (resonant) parametric instability [4, 5] with their subsequent transformation into VLF waves which leave the PW — plasma resonant interaction region and escape into the magnetosphere along the geomagnetic field lines. The remaining issues related to the efficiency of the considered VLF wave generation scheme require separate consideration.

Completing the discussion of the results, we note the conclusion based on the energetic electron precipitation experiments that the region of precipitations along the geomagnetic meridian can reach sizes of up to 1300 km and it is shifted from the Sura facility more to the north than to the south. So large spatial dimensions of the areas with artificial precipitations are still to be explained.

The paper did not discuss the possible effect of the high-energy electron beams precipitating from the Earth’s radiation belt on the ionospheric plasma, which can put it into a turbulent state due to the development of a beam instability or due to the excitation of longitudinal currents [22, 32]. It is also necessary to take into account that VLF waves can be excited by the electrons accelerated in the region with intense plasma turbulence [33, 34]. These issues are of undoubted interest and will be the subject of further research.

In conclusion, we note that the precipitation of high-energy electrons leads to the excitation of atoms and molecules of the Earth’s atmosphere at the ionospheric altitudes, putting them into Rydberg levels. Passing to the lower energy levels, these atoms and molecules radiate in the decimeter- and centimeter-wavelength ranges. In natural conditions, this effect was explored in [35]; recently, it was also detected in the ionosphere modified by high-power radio waves [36, 37]. The impact of artificial generation of microwave radiation on the state of the Earth’s atmosphere is still only to be studied.

The authors thank the Sura facility collaborators for their help in organizing and conducting the experiments. The studies by V. L. Frolov were supported by the Ministry of Education and Science (project No. 3.1844.2017/4.6). The studies by I. A. Bolotin were supported by the Russian Foundation for Basic Research (project No. 17-05-0500475). The studies by A. O. Ryabov were supported by the Russian Foundation for Basic Research (project No. 19-52-15007). Work on the use of the KFU ionosonde Tsyklon was performed by A. D. Akchurin and V. L. Frolov at the expense of a subsidy allocated within the framework of state support to the Kazan (Volga) Federal University in order to increase its competitiveness among the leading world scientific and educational centers.

REFERENCES

1. V. L. Frolov, N. V. Bakhmet’eva, V. V. Belikovich, et al., *Phys. Usp.*, **50**, No. 3, 315 (2007).
2. V. L. Frolov, *Soln.-Zemn. Fiz.*, **1**, No. 2, 22 (2015).
3. V. L. Frolov, *Artificial Turbulence of the Midlatitude Ionosphere* [in Russian], NNSU, Nizhny Novgorod (2017).
4. A. V. Gurevich, *Phys. Usp.*, **50**, No. 11, 1091 (2007).
5. A. V. Streltsov, J.-J. Berthelier, A. A. Chernyshov, et al., *Space Sci. Rev.*, **214**, 118 (2018).
6. L. F. Chernogor, *Physics of High-Power Radio Waves in Geospace* [in Russian], V. N. Karazin National University of Kharkov, Kharkov (2014).
7. G. A. Markov, A. S. Belov, V. L. Frolov, et al., *J. Exp. Theor. Phys.*, **111**, No. 6(12), 916 (2010).
8. V. L. Frolov, V. O. Rapoport, G. P. Komrakov, et al., *JETP Lett.*, **88**, No. 12, 790 (2008).
9. V. L. Frolov, V. O. Rapoport, E. A. Shorokhova, et al., *Radiophys. Quantum Electron.*, **59**, No. 3, 177 (2016).

10. B. E. Bryunelli and A. A. Namgaladze, *Physics of the Ionosphere* [in Russian], Nauka, Moscow (1988).
11. L. F. Chernogor, I. F. Domnin, S. V. Panasenko, V. P. Uryadov, *Radiophys. Quantum Electron.*, **55**, No. 3, 156 (2012).
12. L. F. Chernogor, V. L. Frolov, and V. V. Barabash, *Vestnik PSTU: Telekommun. Radiotekhn.*, No. 2(30), 6 (2016).
13. N. F. Blagoveshchenskaya, *Geophysical Effects in Circumterrestrial Space* [in Russian], Gidrometeoizdat, St. Petersburg (2002).
14. U. S. Inan, T. F. Bell, J. Bortnik, and J. M. Albert, *J. Geophys. Res.*, **108**, No. A5, 1186 (2003).
15. V. V. Belikovich, S. M. Grach, A. N. Karashtin, et al., *Radiophys. Quantum Electron.*, **50**, No. 7, 497 (2007).
16. G. N. Boiko, V. V. Vas'kov, S. F. Golyan, et al., *JETP Lett.*, **39**, No. 11, 652 (1984).
17. J. A. Sauvaud, T. Moreau, R. Maggiolo, et al., *Planet. Space Sci.*, **54**, No. 5, 502 (2006).
18. Ya. Lashtovichka, *Geomagn. Aéron.*, **20**, No. 5, 999 (1989).
19. A. S. Kovtyukh and M. I. Panasyuk, in: *Plasma Heliogeophysics* [in Russian], Fizmatlit, Moscow (2008), Vol. 1, p. 510.
20. E. S. Andreeva, V. L. Frolov, V. E. Kunitsyn, et al., *Radio Sci.*, **51**, No. 6, 638 (2016).
21. H. G. James, V. L. Frolov, E. S. Andreeva, et al., *Radio Sci.*, **52**, 259 (2017).
22. E. V. Mishin, Yu. Ya. Ruzhin, and V. A. Telegin, *Interaction of Electron Beams with Ionospheric Plasma* [in Russian], Gidrometeoizdat, Leningrad (1989).
23. V. L. Frolov, I. A. Bolotin, A. O. Ryabov, and A. D. Akchurin, in: *Abstracts of the XXVI All-Russia Open Scientific Conf. "Radio Wave Propagation," July 1–6, 2019, Kazan* [in Russian], Vol. 2, p. 96.
24. A. O. Ryabov and V. L. Frolov, in: *Abstracts of the XXVI All-Russia Open Scientific Conf. "Radio Wave Propagation," July 1–6, 2019, Kazan* [in Russian], Vol. 2, p. 75.
25. W. F. Utlaut and E. J. Violette, *Radio Sci.*, **9**, No. 11, 895 (1974).
26. P. A. Bespalov and V. Yu. Trakhtengerts, *Alfvén Masers* [in Russian], Inst. Appl. Phys. Rus. Acad. Sci., Gorky (1986).
27. P. P. Belyaev, D. S. Kotik, S. N. Mityakov, et al., *Radiophys. Quantum Electron.*, **30**, No. 2, 189 (1987).
28. V. V. Vas'kov, N. I. Bud'ko, O. V. Kapustina, et al., *J. Atmos. Sol.-Terr. Phys.*, **60**, 1261 (1998).
29. A. Vartanyan, G. M. Milikh, B. Eliasson, et al., *Radio Sci.*, **51**, 1188 (2016).
30. B. Eliasson and K. Papadopoulos, *J. Geophys. Res.*, **113**, A09315 (2008).
31. N. D. Borisov, *Phys. Lett. A*, **206**, 240 (1995).
32. V. N. Oraevsky, *Plasma on the Earth and in Space* [in Russian], Naukova Dumka, Kiev (1980).
33. V. V. Vas'kov, *Radiophys. Quantum Electron.*, **39**, No. 2, 111 (1996).
34. V. V. Vas'kov, G. P. Komrakov, V. N. Oraevsky, et al., *Geomagn. Aéron.*, **35**, No. 1, 154 (1995).
35. V. S. Troitsky, L. N. Bondar', and A. M. Starodubtsev, *Dokl. Akad. Nauk SSSR*, **212**, No. 3, 719 (1973).
36. A. V. Troitsky, V. L. Frolov, A. V. Vostokov, and I. V. Rakut', in: *Abstracts of the XXVI All-Russia Open Scientific Conf. "Radio Wave Propagation," July 1–6, 2019, Kazan* [in Russian], Vol. 2, p. 91.
37. A. V. Troitsky, V. L. Frolov, A. V. Vostokov, and I. V. Rakut', *Radiophys. Quantum Electron.*, **62** (2019) [accepted for publication].